



A biomechanical modelling study of pedestrian skull and brain injury risk in vehicle collisions affected by head rotational speed

XIANGXIAN YI¹, YANGKUN LUO², WU ZHOU¹, JIN NIE^{1,3*}

¹ Loudi Vocational and Technical College, Loudi, China.

² Hunan Automotive Engineering Vocational College, Zhuzhou, China.

³ State Key Laboratory of Advanced Design and Manufacturing Technology for Vehicle, Hunan University, Changsha, China.

Purpose: The purpose of the current study is to investigate the influence of head rotational speed on pedestrian skull and brain injury risk while considering the variation of head linear impact speed and contact location. *Methods:* Pedestrian head-to-vehicle collision simulations are defined by the distributions of pedestrian head-vehicle impact boundary conditions extracted from reconstructions of real-world accidents, where finite element (FE) models of a human body head and vehicle front-end are applied. *Results:* In general, a higher rotational speed at the instant of contacting with vehicle structures leads to a higher skull and brain injury risk: an increase of 30 rad/s in head rotational speed increases the skull fracture risk on average by 2.1–2.6 times and the AIS2+ (Abbreviated Injury Scale) brain injury risk by 1.7–2.7 times in head-hood impacts; for the contacts on the windscreen, the AIS2+ brain injury risk is below 15%, the effect of head rotational speed could be ignored, though an increase of 30 rad/s in head rotational speed leads to 1.6–2.9 times increase in AIS2+ brain injury risk. *Conclusions:* Head rotational speed has significant influences on both skull and brain injury risk. The effect of head rotational speed is always adverse for the risk of brain injuries and hood contact induced skull fractures. However, head rotational speed has no apparent effect on the skull injury risk for head-vehicle contacts at the windscreen.

Key words: biomechanical modelling, vehicle collision, pedestrian skull and brain injury, head rotational speed

1. Introduction

Pedestrian protection in traffic accidents has always been at the forefront of vehicle safety design. Compared to vehicle occupants, pedestrians are vulnerable road users who are at risk of serious head injuries in traffic accidents [5], [21], [32]. Typical pedestrian head injuries include scalp injuries, skull fractures, focal brain injuries (mostly hematoma and contusion) and diffuse brain injuries (mostly diffuse axonal injury and concussion) [26], [27], [33]. Skull fractures and focal brain injuries are usually caused by contact force and linear motion, while rotational motion is the main trigger of diffuse brain injuries [6], [17].

In the past decades, scholars have conducted extensive research on understanding the multiple factors affecting pedestrian head injuries. Otte et al. [22] studied 762 cases of vehicle-to-pedestrian collisions and found that AIS2+ (Abbreviated Injury Scale) head injuries were primarily associated with collision speeds higher than 40 km/h, while a collision speed below this value mainly induced skin soft tissue injuries and concussions, and was associated with a low probability of skull fractures and brain injuries. Mizuno et al. [18] asserted that the risk of head injury depends on the collision speed of the head and the stiffness of the vehicle structures. Peng et al. [23] reported that the probability of AIS2+ and AIS3+ head injury risk for pedestrians was 50% at collision speeds of 39 km/h

* Corresponding author: Jin Nie, Loudi Vocational and Technical College, Loudi, China, State Key Laboratory of Advanced Design and Manufacturing Technology for Vehicle, Hunan University, Changsha, China. E-mail: nie0822@163.com

Received: October 2nd, 2024

Accepted for publication: January 8th, 2025

and 54 km/h, respectively. In a study of head–windshield impact simulations, Wang et al. [31] found that higher initial collision velocities usually lead to larger acceleration peaks, HIC (Head Injury Criterion) and SFC (Skull Fracture Correlate) values, and cause maximum principal strain and von Mises stress to the brain. Recent studies of pedestrian protective measures, such as the sandwich-structure hood [8], [37] and active hood [34], [35], suggested that the pedestrian head injury risk is highly dependent on the contact stiffness. The above publications reveal that head–vehicle contact boundary conditions exert a significant influence on the pedestrian head injury risk. However, most studies on pedestrian head injury only emphasize the effect of linear impact speed, and few scholars have focused on the comprehensive influence of linear and rotational motion. Furthermore, the impactor subsystem tests for pedestrian head protection in new car assessment regulations only consider linear impact speed [3], [4] while ignoring the influence of head rotation motion.

To address the above shortcomings, this study investigates the influences of head rotational speed on pedestrian skull and brain injury risk in vehicle collisions, and also considers the variation of head linear impact speed and contact location. First, the distributions of pedestrian head–vehicle impact boundary conditions, such as head contact location and linear and rotational speed, are extracted from previous reconstructions of real world accidents. Then, head–vehicle impact simulations are conducted using human head and vehicle front FE models, with the definition of representative head linear/rotational speeds and head contact locations. Finally, kinematic-based and biomechanical-based head injury assessment metrics are employed to analyze the comprehensive influences of head–

vehicle impact boundary conditions on the pedestrian skull and brain injury risk.

2. Materials and methods

2.1. Pedestrian head–vehicle contact boundaries

In the current study, the input parameters are selected as the contact location, linear speed and rotational speed of the pedestrian head at the instant of impacting with vehicle hood or windscreen. Particularly, the data observed from previous numerical reconstructions of real-world accidents are extracted following the process illustrated in Fig. 1 [11], [20]. First, real-world vehicle-to-pedestrian crash accidents are selected from the database according to specified inclusion criteria, such as the availability of the information on the vehicle (model and year), the pedestrian (gender, height, weight and age), and the collision configuration (vehicle impact speed, initial contact location, etc.). Then, the multi-body modelling method is employed to simulate crashes, and the optimization algorithm is taken to find the impact configuration parameters that could match the onsite data. In this step, both qualitative and quantitative comparisons between the predicted pedestrian kinematics and corresponding onsite data are performed to validate the quality of each accident reconstruction. Finally, head rotational and linear speed are exported from the accident reconstruction simulations via predefined output options. It should be noted that the current study only retrieved the outputs of

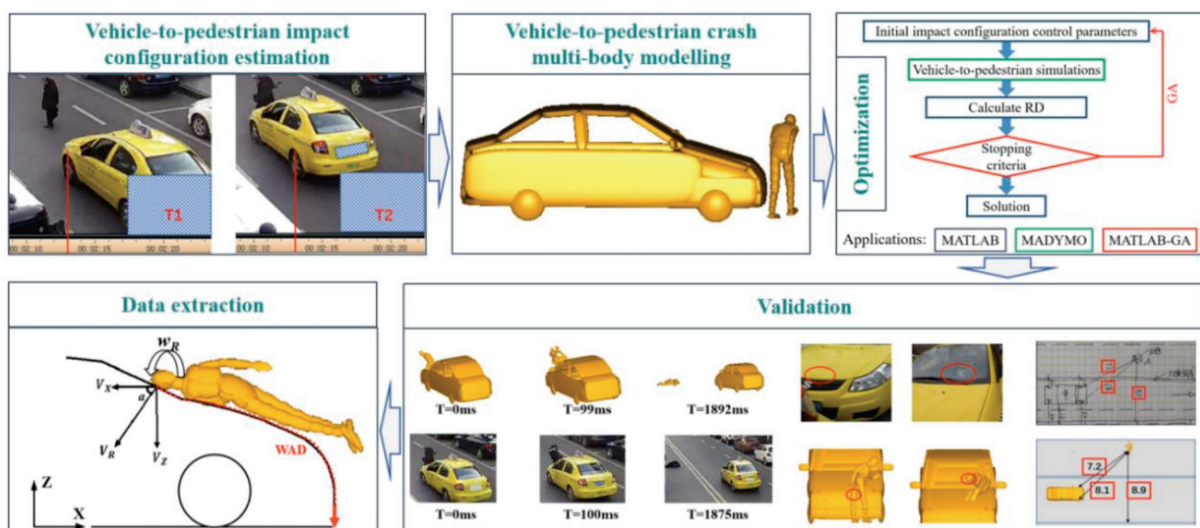


Fig. 1. The process of accident reconstruction and data extraction

these previously performed accident reconstructions with the aim to extract the pedestrian head rotational and linear speed data.

The distributions of pedestrian head contact location, linear speed and rotational speed extracted from accident reconstructions are shown in Fig. 2. The data indicates that the head contact location is mainly on the middle-lower area of the windscreen and the middle-rear area of the hood. In nearly 80% of cases, the head leaner speed is less than 40 km/h, and more than 85% of cases, the head rotational speed is in the range 20–50 rad/s.

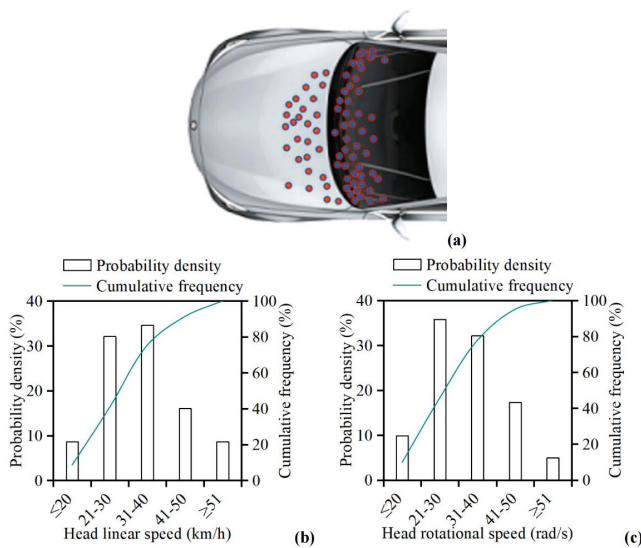
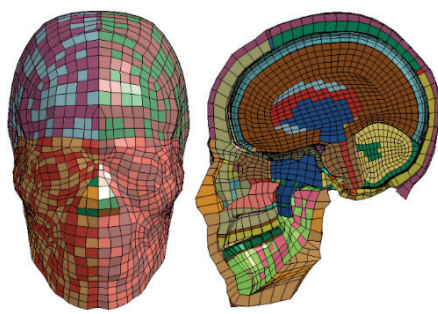


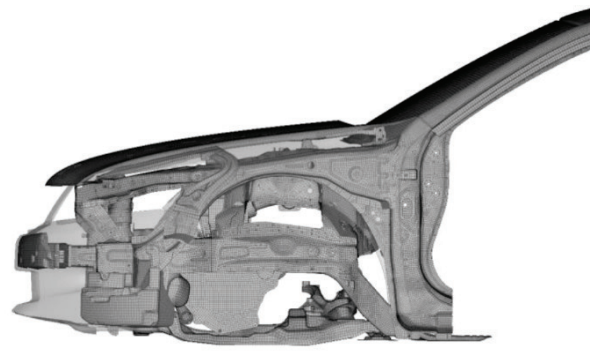
Fig. 2. The distributions of pedestrian head–vehicle contact location (a), linear speed (b) and rotational speed (c) extracted from previous reconstructions of real-world pedestrian accidents

2.2. Human body head and vehicle front FE models

The head model isolated from the THUMS (Total Human Model for Safety) V4.0 pedestrian full-body



(a)



(b)

Fig. 3. Human body head (a) and vehicle front (b) FE models

model (Fig. 3a) was used to predict the skull and brain injury risk in impacts with vehicle front structures (Fig. 3b) which were extracted from the full-size vehicle (2014 Honda Accord) model shared by the NCAC (National Crash Analysis Center). The THUMS model was developed based on the CT and MRI scan data of a 39-year-old male with a height of 173 cm, a weight of 77.3 kg and a BMI of 25.8 [29]. The THUMS head model has detailed anatomical structures, including skin, skull, meninges, CSF (cerebrospinal fluid), white matter, gray matter, brainstem and cerebellum. This model has been validated against cadaver test data in linear and rotational impacts, where the THUMS model could predict plausible response in terms of impact force, acceleration, pressure and brain motion [29]. The THUMS head model has also been widely utilized for biomechanical analysis [2], [15]. The vehicle front model includes a hood (inner and outer panels), engine compartment structures, PVB-glass windscreen, A-pillars and roof compartment. Since the Honda Accord is a typical B-class sedan, it can generally represent mid-size passenger cars on the road. It should be noted that the mechanical property of the windscreen was simulated using the PVB-glass tide connection modelling method and the material parameters which have been validated in the literature [24].

2.3. Head–vehicle impact simulation matrix

To cover the typical head contact locations on the vehicle front observed in accidents (Fig 2a) and the stiffness variation of different vehicle structures, head–vehicle impact simulations were defined at the center and corner of the hood middle-rear area and the windscreen middle-lower area (Fig. 4). Similarly, to cover the main head impact speed range, a linear speed (v) of 20, 30 or 40 km/h combined with a rotational speed (ω) of 20, 30, 40 or 50 rad/s were set to the head model (Fig. 4).

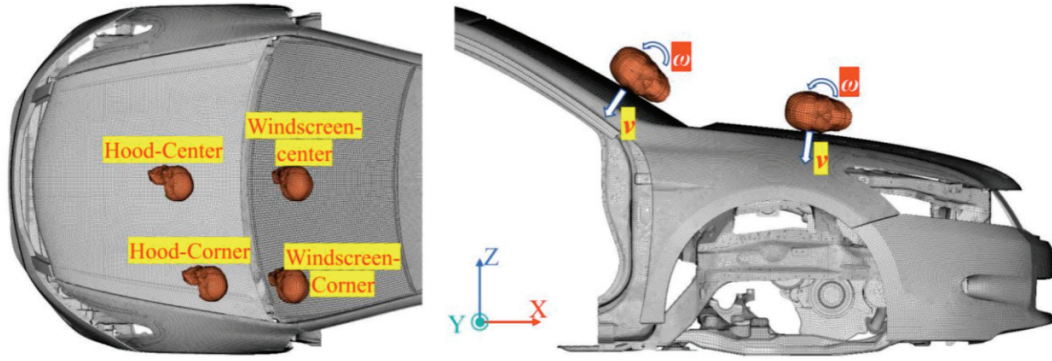


Fig. 4. Head-vehicle impact simulation models (overlapped)

In total, 48 (4 locations*3 linear speeds*4 rotational speeds) head-vehicle impact simulations were defined to represent a range of boundary conditions. In the simulations, the vehicle model was fixed by setting constraints on the longitudinal beams and A-pillars, and a friction coefficient of 0.3 between the head and vehicle structures was defined. Given the fact that pedestrians are mostly struck from the side in accidents, dominated by the head translational movement in the coronal plane (i.e., X - Z plane in Fig. 4) and rotation around the axis in the chest-back direction (i.e., Y -axis in Fig. 4), the linear head speed is set at the X - Z plane and the rotational speed is defined around the Y -axis (passing through the center of mass of the head). This simplified modeling approach for pedestrian head-vehicle impacts has been widely used and accepted in studies of pedestrian head injury [9], [15], [30], [31]. It should be further noted that only the occipital-lateral part of the head is considered as the region contacting with the vehicle model in the simulations, since this part has been observed as the head region mostly contacting with vehicles in accidents [23].

2.4. Head-vehicle impact simulation matrix

The effects of pedestrian head-vehicle contact boundaries on skull fracture and brain injury risk are analyzed using the metrics HIC and maximum principal strain (MPS), respectively. HIC was proposed from cadaver test data for skull fracture assessment, which accounts for both the peak and duration of the head linear acceleration [7]. The formula for HIC calculation is given in Eq. (1), where a_t represents head linear acceleration and $t_2 - t_1$ is 15 ms. To quantitatively estimate the head injury risk, the skull fracture risk curve as a function of HIC (Eq. (2)) developed from the reconstruction of real-world pedestrian accidents [11] and the AIS2+ brain injury risk curve as a function of

MPS (Eq. (3)) proposed by Takhounts et al. [28] are used (Fig. 5). The selection of the injury types and the severity level is made according to epidemiological study findings where skull fractures and AIS2 brain injuries were dominant for pedestrians [13].

$$\text{HIC} = \left\{ \left[\frac{1}{t_2 - t_1} \int_{t_1}^{t_2} a_t dt \right]^{2.5} (t_2 - t_1) \right\}_{\max}, \quad (1)$$

$$P_{\text{skull, fracture}} = 1 - e^{-(\text{HIC}/1519)^{2.32}}, \quad (2)$$

$$P_{\text{AIS2+ brain injury}} = 1 - e^{-(\text{MPS}/0.505)^{2.32}}. \quad (3)$$

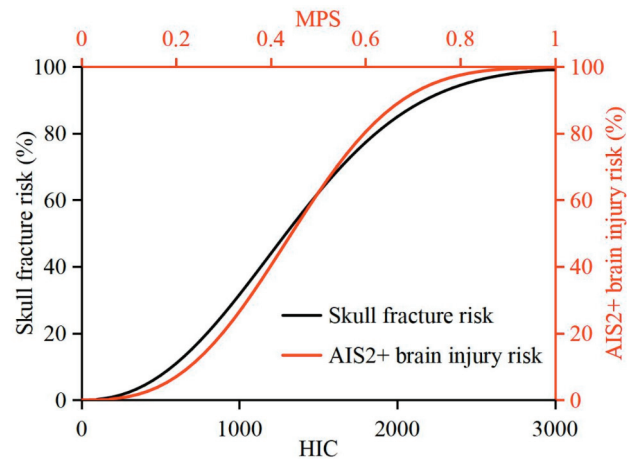


Fig. 5. The injury risk curve for skull fracture as a function of HIC and AIS2+ brain injury as a function of MPS

3. Results

3.1. Skull fracture risk

In Figure 6, the skull stress distribution and head linear acceleration output from the hood and windscreen

corner impacts at 40 km/h are shown. In hood impacts (Fig. 6a), the high-stress area (in red) on the skull and the peak value and width of the head linear acceleration increase with increasing head rotational speed. Meanwhile, for windscreen impacts (Fig. 6b), the high skull stress area is at its maximum in the case with a head rotational speed of 30 rad/s and at its minimum when the head rotational speed is 40 rad/s (no red area). The peak value of head linear acceleration generally

increases with growing head rotational speed, whereas the case of 20 rad/s (the blue line in Fig. 6b) has a wider peak and the case of 30 rad/s (the gray line in Fig. 6b) has a higher second peak.

The HIC values predicted from different simulations are shown in Fig. 7. In hood impacts, the HIC value increases linearly with increasing head rotational speed; on average, the HIC value in the cases of 50 rad/s rotational speed is about 45% higher than

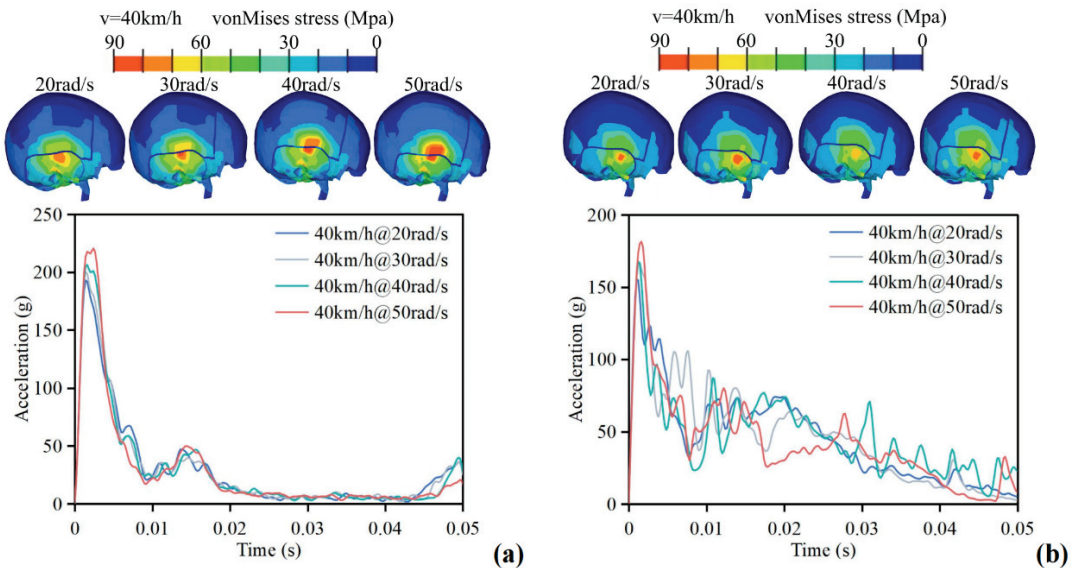


Fig. 6. Skull stress distribution and head linear acceleration (filtered) output from hood (a) and windscreen (b) corner impacts at 40 km/h

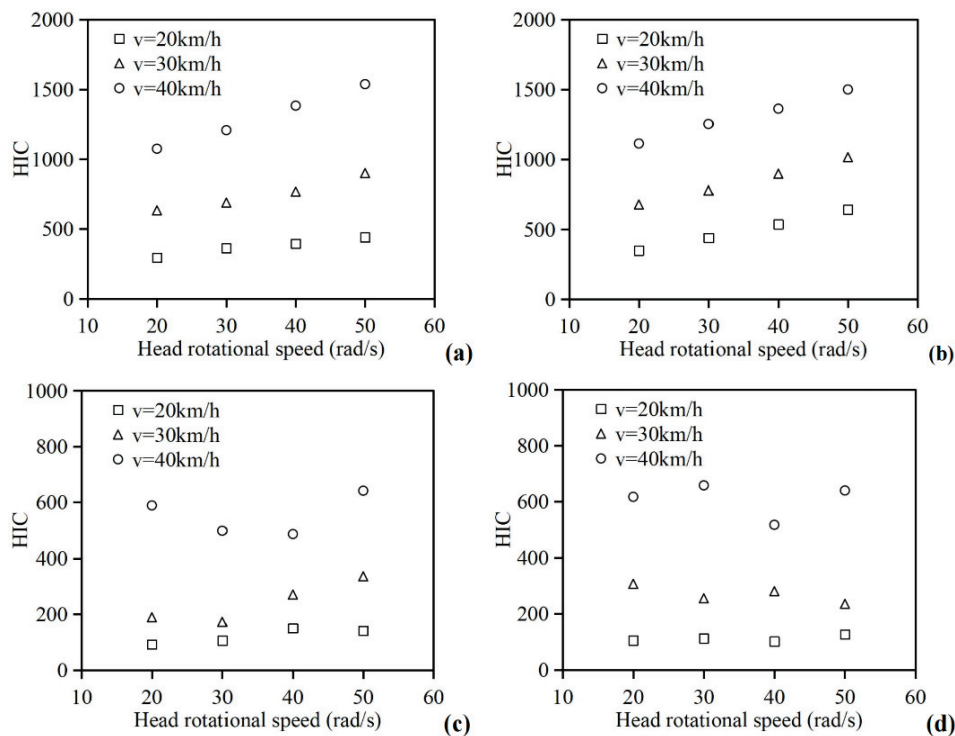


Fig. 7. HIC values predicted from different contact locations: hood center (a), hood corner (b), windscreen center (c) and windscreen corner (d)

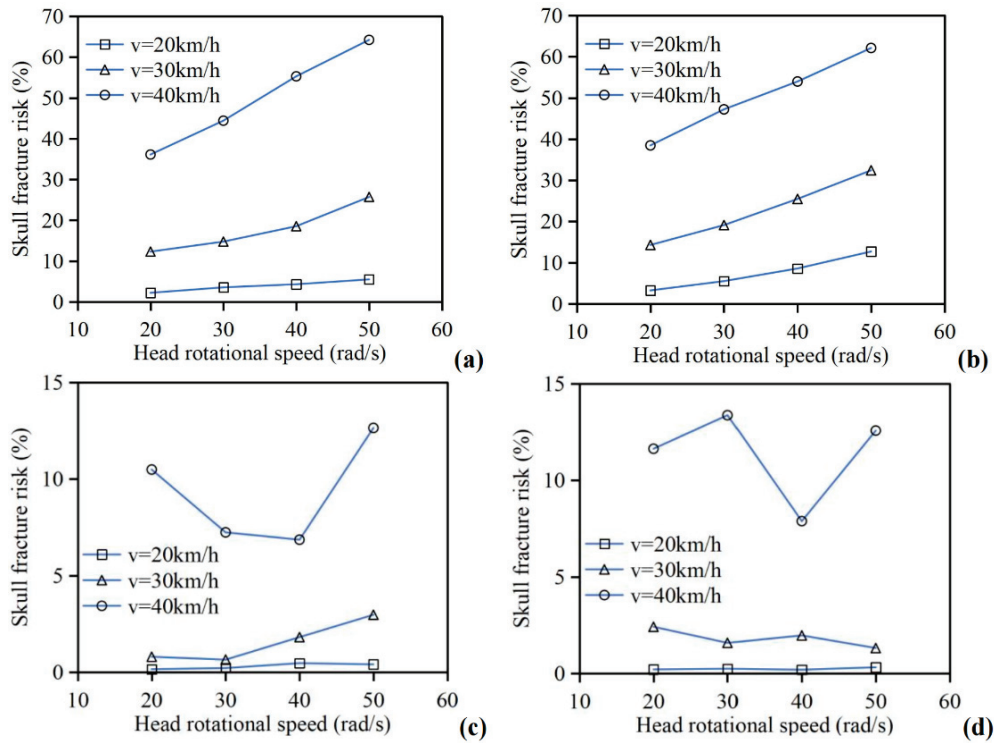


Fig. 8. Skull fracture risk predicted from different contact locations: hood center (a), hood corner (b), windscreen center (c) and windscreen corner (d)

that in the cases of 20 rad/s in head-hood center impacts, and the increase in HIC is 84% when the head rotational speed rises from 20 rad/s (HIC = 348) to 50 rad/s (HIC = 642) in the case where the head impacts with the hood corner at 20 km/h. In head-windscreen impacts, the effect of head rotational speed on HIC is inconclusive. A noticeable trend can be observed from the HIC data, that is, a higher head linear impact speed always leads to a higher HIC, and the HIC is higher in hood impacts than in windscreen contacts.

In Figure 8, the skull fracture risk predicted for different contact locations, which were calculated by the HIC data (Fig. 7) and Eq. 2, is illustrated. In qualitative terms, similar trends as the effects of head linear and rotational speed on HIC are observed for the skull fracture risk. Quantitatively, in hood impacts, the skull fracture risk in the case of 30 km/h@50 rad/s (skull fracture risk = 26–32%) is 2.1–2.3 times of that 30 km/h@20 rad/s (skull fracture risk = 12–14%), and this difference is 1.6–1.8 times between 40 km/h@50 rad/s (skull fracture risk = 62–64%) and 40 km/h@20 rad/s (skull fracture risk = 36–38%). In windscreen impacts, the skull fracture risk is low (<15%) and the effect of head rotational speed could be ignored, although there are variations in the skull fracture risk between different rotational speeds.

3.2. Brain injury risk

In Figures 9 and 10, the typical brain strain distribution and brain MPS from different impacts, respectively are depicted. It can be seen from Fig. 9 that the rotational speed obviously enlarges the strain on the cerebrum (corpus callosum and cerebral internal capsule), while a low rotational speed mainly induces high strain in the cerebellum. The data shown in Fig. 9 further indicate that the brain has more torsion and shear deformation at a higher rotational speed. The simulation data reveal that the brain MPS increases with rising head rotational speed, and the correlation is generally linear in hood impacts. Especially, the brain MPS in the cases with a head rotational speed of 50 rad/s is by about 25% higher than that in the 20 rad/s cases in hood center impacts (Fig. 10a). This value is by about 50% in hood corner impacts (Fig. 10b). In windscreen impacts, the increase in brain MPS induced by rising head rotational speed varies from different head linear speeds and contact locations (Fig. 10c, d). For example, the brain MPS is elevated from 0.13 to 0.19 (increased by 47%) when the head rotational speed increases from 20 to 50 rad/s in the case of contacting with the windscreen center at 20 km/h, while this increase is only 19% for the case where the head impacts with the

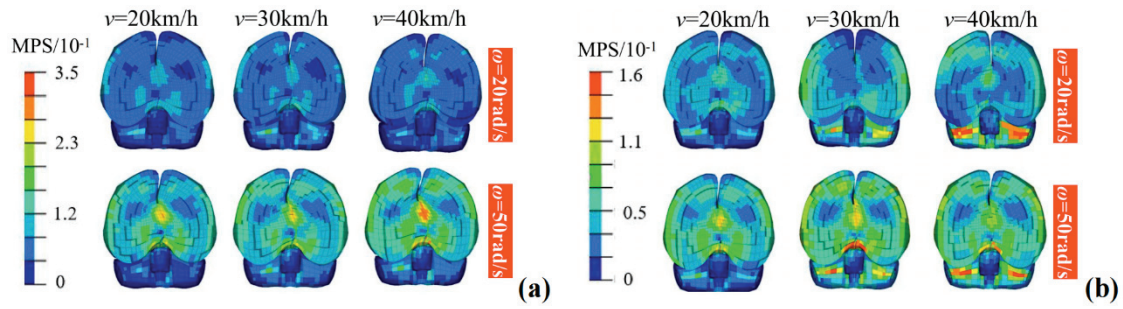


Fig. 9. Typical brain strain distribution predicted from predicted from hood (a) and windscreen (b) impacts

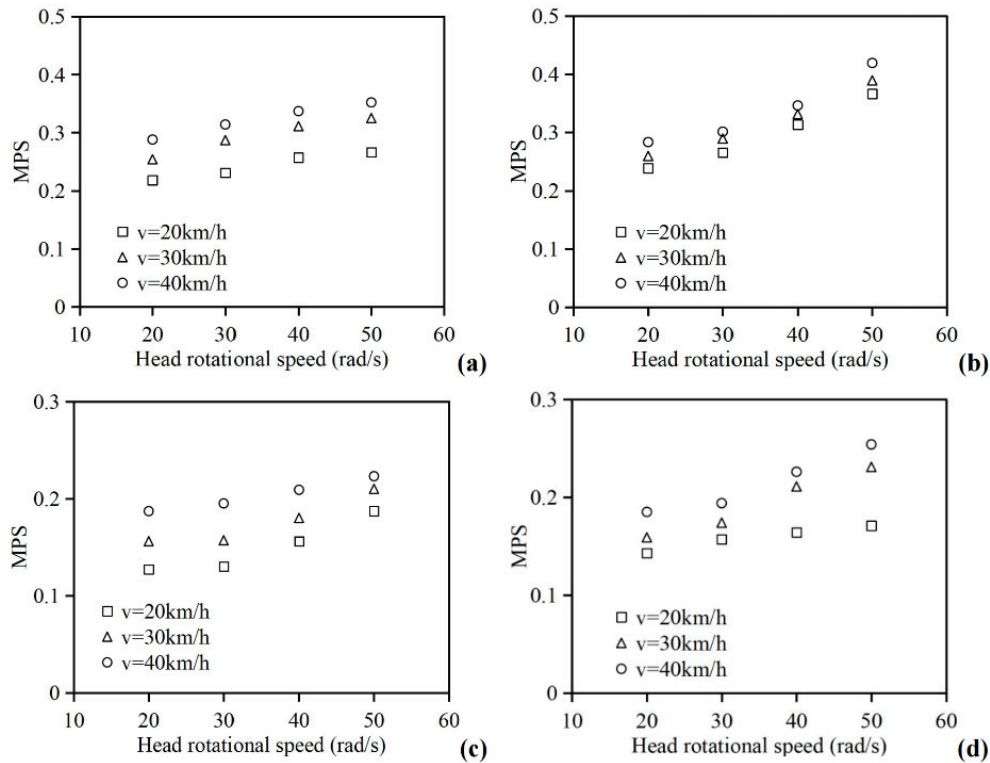


Fig. 10. Brain MPS predicted from different contact locations: hood center (a), hood corner (b), windscreen center (c), and windscreen corner (d)

windscreen center at 40 km/h. The relative increments of brain MPS affected by increasing head rotational speed from 20 to 50 rad/s shift approximately from 20 to 50%. Once again, these data show that a higher head linear speed always leads to a higher brain MPS for a given head rotational speed, and brain MPS is obviously higher in hood impacts than windscreen contacts.

In Figure 11, the predicted AIS2+ brain injury risk calculated from the MPS data (Fig. 10) and Eq. 3 is presented. Similar trends are observed as for MPS, while the relative increase in the AIS2+ brain injury risk induced by increasing head rotational speed from 20 to 50 rad/s reaches an average of 1.7 and 2.7 times for hood center and corner impacts, respectively. The AIS2+ brain injury risk in windscreen contacts is below 15%, the effect of head rotational speed could also be ig-

nored, though an increase of 30 rad/s in head rotational speed leads to 1.6–2.9 times increase in AIS2+ brain injury risk.

4. Discussion

4.1. Main findings

This work uses the head contact boundary conditions extracted from reconstructions of real-world pedestrian accidents as inputs and a human body head model with high biofidelity to define a simulation matrix of head-to-vehicle impacts that includes different head

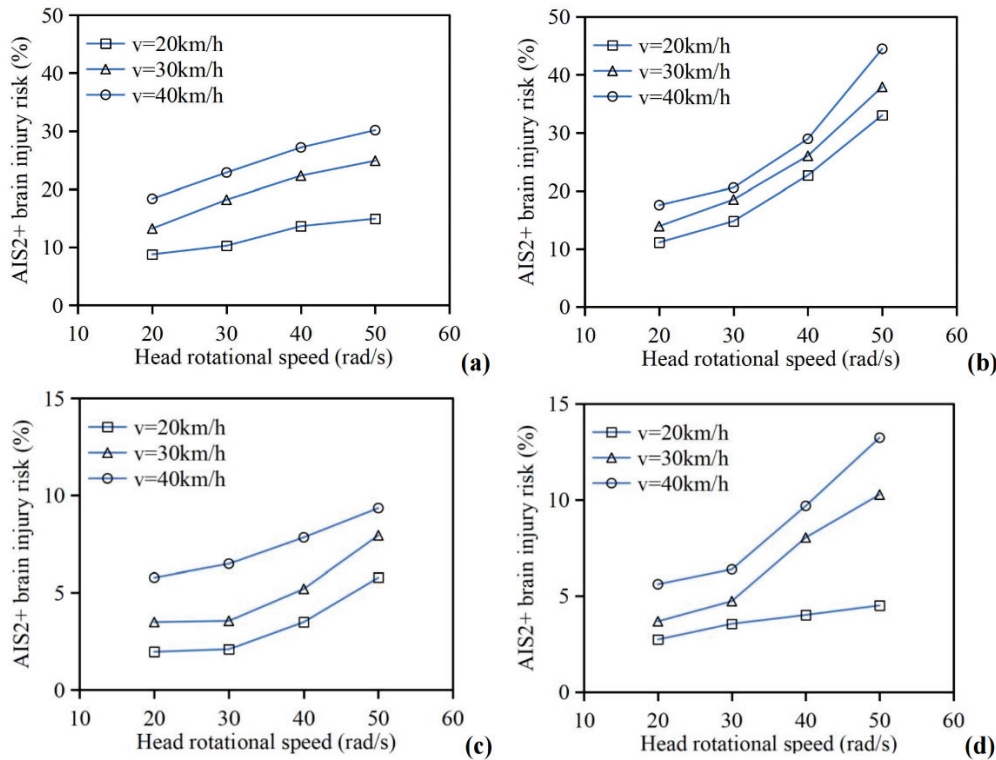


Fig. 11. AIS2+ brain injury risk predicted from different contact locations: hood center (a), hood corner (b), windscreen center (c) and windscreen corner (d)

contact locations and linear and rotational speeds. The rationality and validity of pedestrian head contact linear and angular speed used in the current study could be supported by the following facts. First, the predicted pedestrian head contact linear (25–45 km/h) and angular (35–46 rad/s) speed in reconstructions of accidents crashing around 40 km/h are similar to the results obtained from cadaver collision tests at 40 km/h, where the linear and the rotational speed of pedestrian head at the instant of head-vehicle contact are about 27–50 km/h and 40–50 rad/s, respectively [10]. Second, the consistency between predicted injury and actual injury levels in accident reconstruction [11] can also indirectly reflect the equal relationship between simulated collision loads and real accidents.

The effects of head rotational speed on skull fracture and brain injury risk are analyzed employing the injury criteria HIC and MPS together with the corresponding injury risk curves. The results show that the linear and rotational speed of the head both have significant influences on the skull and brain injury risk. In general, a higher head linear or rotational speed at the instant of contacting with vehicle structures can lead to a higher skull and brain injury risk. It is obvious that the increase in head linear speed can raise the collision energy and hence lead to a higher injury risk.

The effect of head rotational speed on HIC (skull fracture risk) could be understood as its contribution to the rotational kinetic energy and the duration of linear acceleration peak (Fig. 6). However, for windscreen contacts, head rotational speed has no clear effect on the skull injury risk (Fig. 8c and 8d), even though the head linear acceleration peak increases with the rise in head rotational speed (Fig. 6b). This is largely because head rotational speed may also change the head contact stiffness, since the stiffness on the windscreen is sensitive to the impact energy [1]. The simulation results also prove that in windscreen impacts, head rotational speed could influence the peak width of the head linear acceleration (i.e., the duration of the peak, see Fig. 6b), which is an additional factor affecting the HIC value (see Eq. 1). Specifically, the higher injury risk (also higher HIC) in the cases with a lower head rotational speed in windscreen impacts (such as the cases of 40 km/h@20 rad/s shown in Fig. 8c and 8d) arises from the wider peak width of head linear acceleration. Thus, the change in impact energy induced by head rotation, together with the specific stiffness characteristics of the windscreen, result in an uncertain variation pattern of skull fracture risk with the change in head rotational speed. On the other hand, the effect of head rotational speed on the brain injury risk is always adverse (Fig. 9), which has also been de-

scribed as the main factor inducing brain deformation [6], [25], [28].

The simulation results show that an increase of 30 rad/s in head rotational speed can increase the skull fracture risk by an average of 2.6 (2.1) times and the AIS2+ brain injury risk by an average of 2.7 (1.7) times in head-hood corner (center) impacts. By contrast, current pedestrian safety regulations do not consider head rotational speed in the impactor tests [3], [4], and accident data indicates that rotational movement-related brain injuries (concussion and diffuse brain injury) are dominant in pedestrian AIS2+ head injuries [13], although pedestrian safety regulations have significantly reduced the pedestrian head injury risk in accidents by softening the front ends of vehicles [14]. According to the findings of this study, the current impactor tests used in vehicle safety regulations may provide lower estimates of pedestrian head injury risk in real-world accidents. Therefore, it is recommended that the current vehicle safety regulations include head rotational speed, or convert the results that are observed in the tests only considering linear collision velocity to the case where both linear and rotational velocities act simultaneously through an appropriate transfer function.

The comparisons of skull fracture and brain injury risk between head-hood and head-windscreen impacts indicate that, for a given linear and rotational speed, the pedestrian head has a significantly higher injury risk when impacting with the hood than the windscreen (Figs. 8, 11). Taking the impacts at 40 km/h as examples, the HIC values output from head-hood contacts rise from 1000 to 1500, while the HIC values for head-windscreen contacts remain in the range 500–700. These predicted HIC values are similar to real car head impactor test data [19] and numerical simulations [31]. The observed gap in head injury risk between hood and windscreen impacts is also present in previous accident analysis and numerical simulations studies [16], [19]. This is mainly due to the fact that the hood is much stiffer than the windscreen [19]. The head acceleration curves (Fig. 6) also indicate that hood impacts induce a higher and wider peak than contacts with the windscreen, which leads to a higher HIC value and hence a greater head injury risk. Usually, the corner areas of the hood/windscreen are stiffer than the center areas [19], which results in a higher head injury risk for impacts with the corner area for a given linear and rotational speed (Figs. 8, 11). The low head injury risk from windscreen impacts predicted in the current study is in line with the conclusions of a previous work [31], which suggests shortening the hood for a higher proportion of windscreen contacts to re-

duce the pedestrian head injury risk, similar to the safer vehicle front designs proposed in global optimization guidelines [16].

4.2. Limitations

Our study has inevitable shortcomings. Firstly, only one vehicle model was used for the analysis, while the stiffness varying across different vehicle designs may affect the magnitude of the results. However, the general trends observed in the current work are unlikely to be affected by changing the vehicle model, given the relatively consistent stiffness characteristics of hoods and windscreens. Secondly, factors affecting pedestrian head-to-vehicle impact boundaries, such as head contact location (A-pillar, hood and windscreen edge, etc.), head region (forehead and back of the head), and direction of head rotational speed (around the X and Z axes) have not been fully considered. Finally, the FE head model used in the current study could only represent a middle-aged adult, while the enlargement of skull-brain space in the elderly with brain atrophy may exacerbate the role of rotational speed in brain injury risk [36]. The findings of the current work are based on the particularly simulated collisions, changes of impact boundary conditions may affect relationships between head rotational motion and injury risk, and more in-depth analyses are still needed to address brain response under complex loading conditions. Nevertheless, the current study provides the quantified effect of head rotation on skull and brain injury risk under the typical vehicle collision conditions observed from accident reconstructions, which could directly guide the further improvement of vehicle safety assessment methods.

5. Conclusions

The current study aims to enhance our understanding of the comprehensive influences of pedestrian head-vehicle impact boundaries on skull and brain injury risk via FE simulations, with a particular focus on the quantitative effect of head rotational speed. The results indicate that head linear and rotational speed both have significant influences on the skull and brain injury risk. In general, a higher head linear or rotational speed at the moment of contact with vehicle structures will lead to a higher skull and brain injury risk. The effect of head rotational speed is always adverse for the risks of brain injuries and hood contact induced skull

fractures. An increase of 30 rad/s in head rotational speed can increase skull fracture risk by an average of 2.1–2.6 times and the AIS2+ brain injury risk by an average of 1.7–2.7 times in head-hood impacts. However, head rotational speed has no apparent effect on skull injury risk for contacts at the windscreen.

Acknowledgements

This work was supported by Natural Science Foundation of Hunan Province, China (Grant Nos. 2023JJ50512 and 2023JJ50511).

References

- [1] ALVAREZ V., KLEIVEN S., *Importance of windscreen modelling approach for head injury prediction*, Proceedings of the International Research Council on Biomechanics of Injury (IRCOBI) Conference, 2016.
- [2] ATSUMI N., NAKAHIRA Y., TANAKA E., IWAMOTO M., *Human brain modeling with its anatomical structure and realistic material properties for brain injury prediction*, Ann. Biomed. Eng., 2018, 46, 736–748.
- [3] C-NCAP, C-NCAP Management Regulation (2024 Version). China New Car Assessment Programme. China Automotive Technology and Research Center, 2024.
- [4] Euro-NCAP, Vulnerable Road User Testing Protocol, Version 9.1. European New Car Assessment Programme, 2023.
- [5] FAHLSTEDT M., HALLDIN P., KLEIVEN S., *Comparison of multi-body and finite element human body models in pedestrian accidents with the focus on head kinematics*, Traffic Inj. Prev., 2016, 17 (3), 320–327.
- [6] GENNARELLI T.A., OMMAYA A.K., THIBAUT L.E., *Comparison of translational and rotational head motions in experimental cerebral concussion*, SAE Technical Paper, 710882, 1971.
- [7] HERTZ E., *A note on the head injury criterion (HIC) as a predictor of the risk of skull fracture*, Proceedings of the 37th Annals of Advances in Automotive Medicine (AAAM), 1993.
- [8] HOU W., SHEN Y., JIANG K., WANG C., *Study on mechanical properties of carbon fiber honeycomb curved sandwich structure and its application in engine hood*, Compos. Struct., 2022, 286, 115302.
- [9] HUANG J., PENG Y., YANG J., OTTE D., WANG B., *A study on correlation of pedestrian head injuries with physical parameters using in-depth traffic accident data and mathematical models*, Accid. Anal. Prev., 2018, 119, 91–103.
- [10] KERRIGAN J., CRANDALL J., *A comparative analysis of the pedestrian injury risk predicted by mechanical impactors and post mortem human surrogates*, Stapp. Car Crash J., 2008, 52, 08S–018.
- [11] LI G., LIU J., LI K., ZHAO H., SHI L., ZHANG S., NIE J., *Realistic reference for evaluation of vehicle safety focusing on pedestrian head protection observed from kinematic reconstruction of real-world collisions*, Front. Bioeng. Biotech., 2021, 9, 768994.
- [12] LI G., TAN Z., LV X., REN L., *Numerical reconstruction of injuries in a real world minivan-to-pedestrian collision*, Acta Bioeng. Biomech., 2019, 21 (2), 21–30.
- [13] LI G., WANG F., OTTE D., SIMMS C., *Characteristics of pedestrian head injuries observed from real world collision data*, Accid. Anal. Prev., 2019, 129, 362–366.
- [14] LI G., WANG F., OTTE D., CAI Z., SIMMS C., *Have pedestrian subsystem tests improved passenger car front shape*, Accid. Anal. Prev., 2018, 115, 143–150.
- [15] LI G., XU S., XIONG T., LI K., QIU J., *Characteristics of head frequency response in blunt impacts: A biomechanical modeling study*, Front. Bioeng. Biotech., 2024, 12, 1364741.
- [16] LI G., YANG J., SIMMS C., *Safer passenger car front shapes for pedestrians: a computational approach to reduce overall pedestrian injury risk in realistic impact scenarios*, Accid. Anal. Prev., 2017, 100, 97–110.
- [17] MARGULIES S., THIBAUT L., GENNARELLI T., *Physical model simulations of brain injury in the primate*, J. Biomech., 1990, 23 (8), 823–836.
- [18] MIZUNO K., KAJZER J., *Head injuries in vehicle-pedestrian impact*, SAE Technical Paper, 2000-01-0157, 2000.
- [19] MIZUNO K., YONEZAWA H., KAJZER J., *Pedestrian headform impact tests for various vehicle locations*, Proceedings of the 17th International Technical Conference on the Enhanced Safety of Vehicles (ESV), Amsterdam, the Netherlands, ESV Paper No. 278, 2001.
- [20] NIE J., LI G., YANG J., *A study of fatality risk and head dynamic response of cyclist and pedestrian based on passenger car accident data analysis and simulations*, Traffic Inj. Prev., 2014, 16 (1), 76–83.
- [21] OTTE D., JÄNSCH M., HAASPER C., *Injury protection and accident causation parameters for vulnerable road users based on German In-Depth Accident Study GIDAS*, Accid. Anal. Prev., 2012, 44 (1), 149–153.
- [22] OTTE D., *Severity and mechanism of head impacts in car-to-pedestrian accidents*, Proceedings of the International Research Council on Biomechanics of Injury (IRCOBI) Conference, 1999.
- [23] PENG Y., CHEN Y., YANG J., OTTE D., WILLINGER R., *A study of pedestrian and bicyclist exposure to head injury in passenger car collisions based on accident data and simulations*, Safe Sci., 2012, 50 (9), 1949–1959.
- [24] PENG Y., YANG J., DECK C., WILLINGER R., *Finite element modeling of crash test behavior for windshield laminated glass*, Int. J. Impact. Eng., 2013, 57 (7), 27–35.
- [25] ROWSON S., DUMA S., BECKWITH J., CHU J., GREENWALD R., CRISCO J., BROLINSON P., DUHAIME A.-C., MCALISTER T., MAERLENDER A., *Rotational head kinematics in football impacts: an injury risk function for concussion*, Ann. Biomed. Eng., 2011, 40 (1), 1–13.
- [26] SCHMITT K.U., NIEDERER P.F., MUSER M.H., WALZ F., *Trauma biomechanics*, Third edition, Springer, 2010.
- [27] SIMMS C., WOOD D., *Pedestrian and Cyclist Impact*, Springer, 2009.
- [28] TAKHOUNTS E., CRAIG J., MOORHOUSE K., MCFADDEN J., HASIJA V., *Development of brain injury criteria (BrIC)*, Stapp. Car Crash J., 2013, 57, 243–266.
- [29] Toyota Motor Corporation, Documentation: Total Human Model for Safety (THUMS), AM50 pedestrian/occupant model advanced version 4.0 20111003, 2011.
- [30] WANG F., PENG K., ZOU T., LI Q., LI F., WANG X., WANG J., ZHOU Z., *Numerical reconstruction of cyclist impact accidents: Can helmets protect the head-neck of cyclists*, Biomimetics, 2023, 8, 456.
- [31] WANG J., WANG R., GAO W., CHEN S., WANG C., *Numerical investigation of impact injury of a human head during*

- contact interaction with a windshield glazing considering mechanical failure*, *Int. J. Impact Eng.*, 2020, 141, 103577.
- [32] WHO. Global status report on road safety 2023. World Health Organization, Geneva, Switzerland, 2023.
- [33] YANG J., *Review of injury biomechanics in car-pedestrian collisions*, *Int. J. Veh. Saf.*, 2005, 1 (1–3), 100–117.
- [34] YANG Z., DENG T., ZHAN Z., *Design and analysis of vehicle active hood for pedestrian protection*, SAE Technical Paper, 2021-01-7019, 2021.
- [35] ZHAN Z., LV F., RAN X., ZHOU G., ZHAO S., HE X., WANG J., LI J., *Automotive hood design based on machine learning and structural design optimization*, SAE Technical Paper, 2023-01-0744, 2023.
- [36] ZHOU Z., LI X., KLEIVEN S., *Biomechanics of acute subdural hematoma in the elderly: A fluid-structure interaction study*, *J. Neurotraum.*, 2019, 36 (13), 2099–2108.
- [37] ZOU T., CHEN D., LI Q., WANG G., GU C., *A novel straw structure sandwich hood with regular deformation diffusion mode*, *Compos. Struct.*, 2024, 337, 118077.